



## Research article

## Rare earth elements - Source and evolution in an aquatic system dominated by mine-Influenced waters

Patrícia Gomes<sup>a</sup>, Teresa Valente<sup>a,\*</sup>, Rosa Marques<sup>b</sup>, Maria Isabel Prudêncio<sup>b</sup>, Jorge Pamplona<sup>a</sup><sup>a</sup> Campus de Gualtar, Institute of Earth Sciences, Pole of University of Minho, Universidade do Minho, 4710-057 Braga, Portugal<sup>b</sup> Centro de Ciências e Tecnologias Nucleares (C2TN), Departamento de Engenharia e Ciências Nucleares (DECN), Instituto Superior Técnico, EN 10 (km 139.7), 2695-066 Bobadela, Portugal

## ARTICLE INFO

## Keywords:

Rare earth elements  
Acid mine drainage  
Iberian pyrite belt  
Aquatic system degradation  
Water scarcity

## ABSTRACT

Acid mine drainage (AMD), formed by the instability of sulfides, typically generates acidity and releases potentially toxic elements and sulfate to the environment, among other pollutants. An example is the group of rare earth elements (REE) that may have high toxic behavior. This toxicity leads to degradation of soils, water reservoirs and rivers, promoting serious risks for the ecosystems. So, the main goal of the present work is to study the hydrochemical properties of a system with mine-influenced waters during the rainy season, focusing on the origin, evolution/behavior, and concentration of REE. The study area is the São Domingos mining complex, located in one of the largest metallogenetic provinces in the world (Iberian Pyrite Belt), known by the evidences of AMD contamination. The obtained results reveal extraordinarily low pH (0.4), high electrical conductivity, reaching 26,200  $\mu\text{S}/\text{cm}$ , and high values of sulfate and acidity. Regarding the REE, the determined concentration exceeded that observed in normal pH of neutral freshwaters by 2–3 times the order of magnitude. The results revealed that Y and Ce are distinguished in practically all sampled sites, due to its higher concentrations, with maximum values of 221.8 and 166.9  $\mu\text{g}/\text{L}$ . In general, the concentrations increase as the water pH decreases. The statistical analysis indicates that REE elements may have a common origin, mutual dependence, and similar behavior during transport with typical AMD elements and composition of host rocks. Most samples show enrichment in middle REE (MREE) (Gdn/Lun), like the classic signature of AMD. In turn, colloids and AMD-precipitates may be participating in the incorporation of these elements. Therefore, due to potential risk of impacts on ecosystems, REE are a topic of relevant interest for future studies in order to assist monitoring processes and help government decisions related to water quality management.

## 1. Introduction

Raw materials are essential for efficient functioning of the world economy, being preponderant in maintaining levels of current societies development (e.g., Gomes, 2021). Nowadays, some mineral resources assume a critical nature, due to its importance in strategic industries (e.g. electronic devices), technological development, and energy transition processes (Massari and Ruberti, 2013). However, minerals must be mined, and mining activity exhibits serious conflicts with nature preservation (Gomes, 2011). This situation generated millions of contaminated hectares with mining wastes, often without any type of control (Fernández-Caliani et al., 2009; Thornton, 1996). This contamination results in general degradation of soils, water reservoirs and rivers, leading to serious risks for humans, animals, plants, and ecosystems

(EPA, 2012). An example is related to the rare earth elements (REE) that are considered of extreme importance in today's society, however they might have high toxic behavior (Balaram, 2019; Protano and Riccobono, 2002).

Several authors (e.g., Gwenzi et al., 2018; Huang et al., 2016; Kulaksiz and Bau, 2007; Kurvet et al., 2017; Migaszewski and Galuszka, 2015; Tao et al., 2022) consider REE as emerging pollutants, and as such, they trigger concern with the increase of its use and interaction with the environment. In terms of health risk, problems with kidney dysfunction, reproductive deficiencies, mental retardation or even death were reported (El Rasafi et al., 2021). The work by Rim (2016) presents a literature review on the environmental impacts and REE-induced effects on human health.

The REE group includes the yttrium, scandium, and other fourteen

\* Corresponding author.

E-mail address: [teresav@dct.uminho.pt](mailto:teresav@dct.uminho.pt) (T. Valente).<https://doi.org/10.1016/j.jenvman.2022.116125>

Received 4 July 2022; Received in revised form 16 August 2022; Accepted 25 August 2022

Available online 5 September 2022

0301-4797/© 2022 The Authors. Published by Elsevier Ltd. This is an open access article under the CC BY-NC-ND license (<http://creativecommons.org/licenses/by-nc-nd/4.0/>).

metals, which represent the so-called lanthanides (e.g., Du and Graedel, 2011). In a simplistic approach, REE can be divided into three subgroups: LREE (light REE), HREE (heavy REE), and MREE (middle REE) (e.g., Dukov, 2007). They occur in low concentrations in natural waters however, previous works have shown high concentrations of these elements in acidic systems (Åström and Corin, 2003; Noack et al., 2014; Verplanck et al., 2004). Acid mine drainage (AMD), formed by the instability of sulfides in the presence of weathering agents (mainly water and oxygen) (Valente et al., 2012, 2015), is normally associated with metals and coal deposits. Through a series of biogeochemical reactions, sulfide-rich wastes generate acidity, and release potentially toxic elements (PTE), and sulfate to the environment, among other pollutants (Gomes, 2021). Thus, the REE in these contexts are characterized by poor mobility and separation during weathering, being considered indicators of the geochemical processes (Li and Wu, 2017). Therefore, they can help to understand the geochemical evolution of an aqueous system, having been used over the last decades to investigate water-rock interactions (e.g., Olías et al., 2005; Zhao et al., 2007; Pérez-López et al., 2010; Sahoo et al., 2012; Grawunder et al., 2014; Migaszewski et al., 2014). In addition, the ability to preserve the original geochemical characteristics allows them to be used to identify possible sources of pollution (He et al., 2010; Delgado et al., 2012) and restrict the processes that control fate and subsequent mobilization of REE (Pérez-López et al., 2010; Sharifi et al., 2013). However, few studies are focused on REE from AMD sources in sulfide mining areas (González et al., 2020).

In a similar way to what is happening throughout Europe, rehabilitation measures are being implemented in several mines in the Iberian Pyrite Belt (IPB), namely in São Domingos complex ([www.edm.pt](http://www.edm.pt)). These rehabilitation projects aim to contribute to minimizing the environmental impact and promoting the ecosystems' sustainability. Consequently, the inventory and study of surface water bodies, as well as assessment of the contamination degree regarding elements of high interest and demand, such as REE, are currently a strategic opportunity (Costis et al., 2021). Furthermore, considerable attention is being created due to potential recovery of REE in AMD scenarios (e.g., Hermassi et al., 2022; Pérez-López et al., 2010; Zhang and Honaker, 2020).

Although the literature about REE in aquatic ecosystems refers mainly to uncontaminated freshwaters (Galhardi et al., 2022), acquiring knowledge about the geochemical behavior of REE in mine waters is vital for the promotion of the ecological quality. Therefore, this need for better understanding of REE dynamics in mine waters states the novelty of the present study, especially in a context of climate change (Gomes et al., 2018), in which water management is a topic of urgent concern. So, the present work intends to study the hydrochemical properties based on six campaigns during the rainy season, in a region facing water scarcity. Specific aims are focused on the source, evolution/behavior, and concentration of REE, in a mining area with strong evidence of AMD contamination.

## 2. Study area

The IPB is one of the largest metallogenic provinces in the world, but it is also one of the driest regions in Europe, having to face problems of water quantity and quality (Gomes et al., 2018). Positioned in a Mediterranean context, it constitutes a vast geographical area in the south of the Iberian Peninsula, approximately 250 km long and 30–50 km wide.

The entire metallogenic province has a high density of polymetallic sulfide mines being a decisive source of base and precious metals (e.g., Cu, Zn, Pb, Sn, Ag, Au, Fe, Co, Cd) (Matos et al., 2006a, b; Matos and Martins, 2006; Matos et al., 2012), promoting the degradation of aquatic systems. Consequently, mining activity can limit the water uses in the watersheds where the ore deposits are located (e.g., Gomes et al., 2020). It should be noted that these problems are experienced in many other countries with mining tradition and that currently suffer from water

scarcity phenomena (e.g., Anawar, 2015). The São Domingos deposit is in the South Portuguese Zone (SPZ) of the Hesperic massif. The geological materials are of volcanic and sedimentary origin and have ages ranging from the Devonian to the Carbonic, being constituted by three main litho-stratigraphic units: Philite-Quartzitic Group; Mértola Formation; Vulcano-Sedimentary Complex (VSC) (e.g., Matos, 2004; Matos et al., 2006b; Oliveira and Matos, 2004) (Fig. 1).

São Domingos is one of the largest and most emblematic mines in IPB, having closed without any kind of environmental control, in 1966. It is currently undergoing rehabilitation (since 2017). Inserted in the Gadiana hydrographic basin, it is intersected by three water lines: Cabeça de Aires, São Domingos and Mosteirão stream. The Cabeça de Aires stream feeds the Tapada Grande dam, located upstream from the mining complex, serving for water supply and recreation. The São Domingos stream runs through the mining area, intersecting the Mosteirão stream at the point immediately following the mine. The Chança River is the main receiver of the water streams that drain the slopes of the numerous waste-dumps (Batista, 2000).

The water channels show typical red coloration, efflorescent salts, ochre precipitates, and colloidal particles, corresponding to evident signs of AMD (Gomes et al., 2017a, 2020) (Fig. 2).

The climate of the region can, generally, be considered as dry sub-humid (Gomes, 2021). Climate data reveals that in recent years there has been a considerable reduction in precipitation (minimum of 203 mm) and an increase in the average annual temperature (16.5 °C), these variations coinciding with the sampling period for these work (2016/2017) (Gomes, 2021).

Among European countries, Portugal is more vulnerable to the impacts of climate change. Drought phenomena, which have been intensifying over the years, as well as the high temperatures experienced, are the cause of numerous events that enhance extreme contamination (Gomes et al., 2018).

## 3. Materials and methods

### 3.1. Sampling and analytical methods

The drainage waters represent the result of the water contact with the lithologies present in the mining area and in the waste-dumps, so that their properties might indicate the conditions for the pollutants mobilization. Thus, the water sampling sites were selected considering different environmental conditions. Each location is representative of aspects such as hydrology, water use, mining location, reservoir nature, stream, or pit lake (Fig. 3), among other factors. Monthly campaigns were carried out from October 2016 to March 2017, to represent the rainy season, corresponding to the hydrological year of 2016/2017.

The 12 sampling sites and their description are presented below (Fig. 3):

- PAT1 – site located in the Tapada Grande reservoir, upstream of the mining area, being used for recreational purposes;
- PAT2 – pit lake;
- PAT3 to PAT9 – sites along the river path that are directly influenced by AMD and waste dumps, including acidic lagoons;
- PAT10 – site located immediately at upstream of the confluence with the Chança River;
- PAT11 – AMD dispersion plume in the river, being a moving point throughout the year;
- PAT12 – Chança reservoir, being used for irrigation and to produce drinking water.

The collection of samples was carried out in the superficial portion proceeding simultaneously with the *in-situ* measurement of pH, temperature, and electrical conductivity (EC). These parameters were determined with a multiparameter equipment, Orion Brand, Star 5 model.

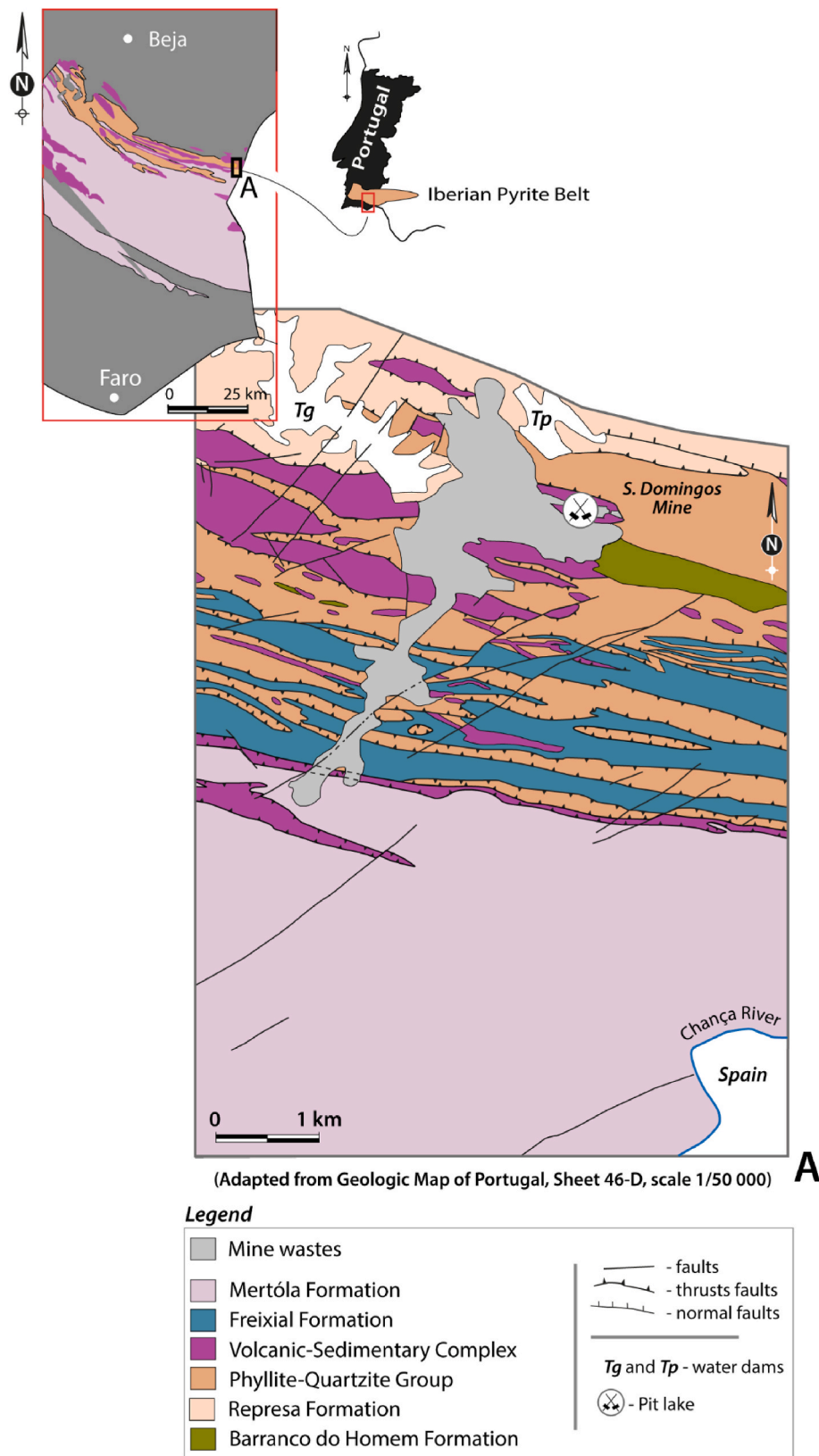


Fig. 1. Portuguese sector of the Iberian Pyrite Belt, with focus in São Domingos deposit.

At each location, 1 L of sample was collected in high-density polyethylene bottles (Kartel bottles). For analysis of the REE, a 50 mL aliquot was filtered using a PET syringe and disposable disc with a 0.45 µm pore-diameter PES (polyestersulfone) filter, and acidified with HNO<sub>3</sub>, 65%

suprapur Merck, to preserve the sample at pH less than 2 (Standard Methods 3010B). Storage vials were properly prepared in accordance with ASTM 5245 (ASTM, 1992).

At the laboratory, the REE were analyzed using inductively coupled



Fig. 2. Accumulation of ochre precipitates (a) with colloidal properties along channel bed (b).

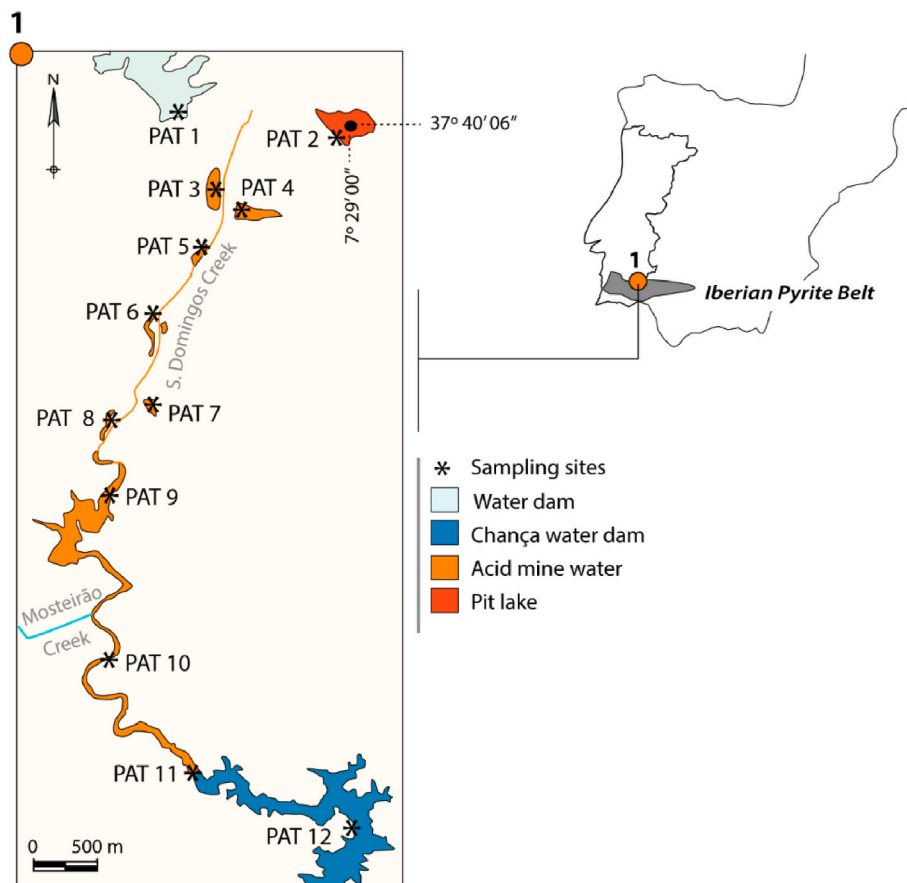


Fig. 3. Location of sampling sites along the river system - PAT1 to PAT12 (adapted from Cordeiro, 2017).

plasma-mass-spectrometry (ICP-MS), while total acidity and sulfate were determined by volumetric titration (Standard Methods 2310 B) and turbidimetry (Standard Methods 4500 E), respectively.

### 3.2. Statistical analysis and data treatment

The data was subjected to normalization obtained through calculation between the value used to normalize, the average and the standard deviation. The box and whiskers plots of expeditious parameters (pH, EC), acidity and sulfate were obtained by using the SPSS Release 25.0 software. The factor analysis used to highlight the correlation between

physicochemical parameters was performed using normalized varimax rotation and the main components, that is, the number of extracted factors, selected based on the Bartlett method. The analysis of the correlation coefficients was performed based on the Spearman method. Sample data for REE were normalized to the Post Archean Australian Shale (PAAS) (Taylor and McLennan Blackwell, 1985).



### 4. Results and discussion

#### 4.1. Hydrochemical properties

Fig. 4 represents the box and whiskers plots of parameters measured *in situ*, as well as acidity and sulfate, thought as essential indicators of AMD quality (e.g., García-Lorenzo et al., 2016). The results reveal that the highest pH value (7.48) corresponds to the clean water storage dam, Tapada Grande (PAT 1), in October 2016, showing the absence of mining contamination. In turn, PAT7 represents a site with an extraordinarily low pH (0.4), recording here the minimum value for this parameter.

Regarding electrical conductivity (EC), the minimum value of 26.50  $\mu\text{S}/\text{cm}$  was obtained in the Chança reservoir (PAT12) in January 2017, while the maximum EC occurred in PAT 7, reaching 26,200  $\mu\text{S}/\text{cm}$ , in November 2016.

The results obtained for these two parameters (pH and EC) are in accordance with the nature of the sampled environments, that is, the reservoirs with clean water had the highest pH, while the respective EC values were the lowest. The samples from the pit lake (PAT2) and acidic lagoons (PAT3 to PAT10) presented pH average values below 3, which confirms the influence of leachates from sulfide-rich waste. From the point of dispersion of AMD plume in the river (PAT11), there is a tendency for an increase in pH and a decrease in EC, provided by the distance from the waste accumulations, and consequent natural attenuation effects, for example, by dilution and formation of AMD-precipitates. This justifies the lowest EC value of 26.50  $\mu\text{S}/\text{cm}$ , measured in PAT12.

The results obtained for acidity revealed that the samples located in the pit lake (PAT2) and along the river system (PAT3 to PAT11) were acidic in most campaigns; however, in conditions of high precipitation and consequent dilution, pH value can increase, resulting in alkalinity production. These results were observed at sampling sites PAT6, PAT8 and PAT11. It can be clearly seen that PAT7 (acidic lagoon – Achada do Gamo), PAT5 (acidic lagoon), and PAT2 (pit lake) are the sites with the highest acidity concentrations, following the behavior already described

for pH and EC. The higher acidity at PAT7 is consistent with the influence of the most reactive wastes already identified (Cordeiro, 2017; Gomes et al., 2021), in the vicinity of this point. Sulfate concentrations exhibit a similar behavior to acidity. Therefore, the sites with the highest contents of this anion are PAT7, PAT2, and PAT5.

In summary, the parameters measured *in situ*, particularly pH, combined with those of total acidity and sulfate, clearly indicate typical conditions of AMD contamination (Dold, 2014; Moreno-González et al., 2022; Soyol-Erdene et al., 2018). These results show that PAT1 and PAT12 are clean water points, as indicated by the lowest concentrations, with the remaining points being in transitional conditions (PAT3 to PAT11). In general, except for PAT7, there is a decrease in the sulfate concentration along the river path, that is, there is attenuation as one moves downstream, a likely function of the dilution effect and of sulfate fixation in neoformations such as jarosite, precipitated in the channel bed (Gomes et al., 2017a).

Despite this, at the point located immediately at upstream of the confluence with the Chança river (PAT10), the average concentration of sulfate remains high, reaching 1451.7 mg/L.

Regarding to the REE, the six months of campaigns, related to the rainy season, are analyzed, and discussed below (Table 1) in terms of concentration of each element and correlation with other parameters (Table 2).

The statistical results reveal that PAT1 and PAT12 have values usually below the detection limit of the analytical method. As mentioned above, these two sites correspond to clean water (water dams). The same does not apply to other sites, which correspond to pit lake and points along the river system. In the same way as observed for other indicators, PAT2 and PAT7 also show the highest concentrations of REE.

Regarding the elements Y and Ce, they are distinguished in practically all sites by the higher concentrations, with maximum values (in PAT2) of 221.8 and 166.9  $\mu\text{g}/\text{L}$ , respectively. According to the study by Soyol-Erdene et al. (2018), Ce seems to occur at high concentrations in AMD environments.

In general, the REE concentrations increase as the pH decreases (Fig. 5). Such inverse relationship has previously been reported in AMD

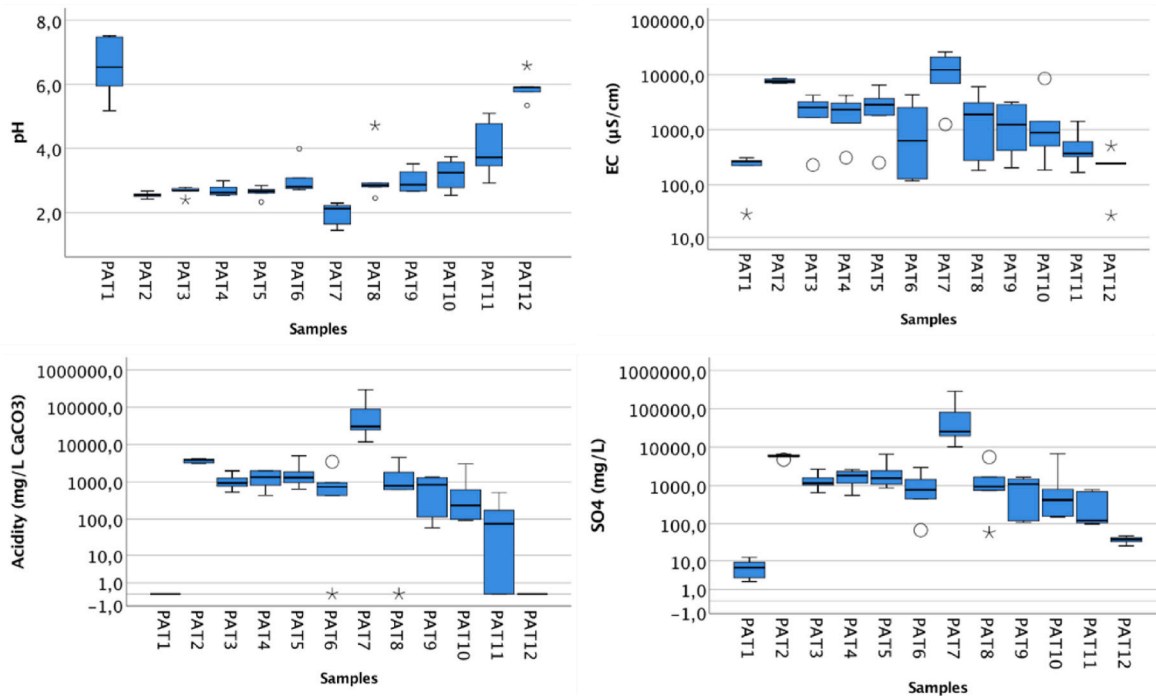


Fig. 4. Box and whiskers plots of expeditious parameters (pH and electric conductivity – EC), acidity, and sulfate, collected over 6 campaigns. The length of the box shows the interquartile range, while the horizontal line inside the box represents the average value. The whiskers are lines that extend from the box to the highest and lowest, excluding outliers, which represent extreme (star symbol) or mild outliers (circle symbol).

**Table 1**

Statistical summary of REE (in µg/L) over six campaigns (from October to March). Avg = Average; Min = Minimum; Max = Maximum; SD=Standard Deviation. Detection limit (DL) = 1.0 µg/L.

		Sc	Y	La	Ce	Pr	Nd	Sm	Eu	Gd	Tb	Dy	Ho	Er	Tm	Yb	Lu
PAT1	Avg	1,1	<DL	<DL	<DL	<DL	<DL	<DL	<DL	<DL	<DL	<DL	<DL	<DL	<DL	<DL	<DL
	Min	<DL	<DL	<DL	<DL	<DL	<DL	<DL	<DL	<DL	<DL	<DL	<DL	<DL	<DL	<DL	<DL
	Max	1,4	<DL	<DL	<DL	<DL	<DL	<DL	<DL	<DL	<DL	<DL	<DL	<DL	<DL	<DL	<DL
	SD	0,2	-	-	-	-	-	-	-	-	-	-	-	-	-	-	-
PAT2	Avg	64,6	221,8	61,9	166,9	24,1	125,6	40,7	10,9	59,9	9,5	44	9,3	21,5	5,4	16,9	5,2
	Min	49,4	186	51,3	142	20	107	33,7	10	50,9	8,7	37,2	8,3	18,1	2,9	14,3	2,6
	Max	77	266,2	74,9	199	29,4	149,7	48,9	12,7	70,6	10,4	52	10	25,5	10	19,9	10
	SD	10,5	31,1	8,7	20,9	3,3	15,9	5,6	-	7,1	0,7	5,5	0,8	2,7	3,6	2	3,7
PAT3	Avg	20	61,2	22	54,6	7	31,5	8,6	2,3	13,2	2	11,1	2,1	6,3	1,2	5,1	1,1
	Min	10,5	32,6	11,5	28,6	3,7	17,2	4,7	1,2	7,2	1,1	6,4	<DL	3,7	<DL	3	<DL
	Max	28,4	96,9	36,3	85,3	11,4	49,1	13,9	4,1	20,9	3,6	17,4	4,1	10,1	1,9	8,3	1,8
	SD	8,6	22,9	8,6	19,6	2,7	11,1	3,2	-	4,8	0,9	3,9	1,1	2,3	0,4	1,9	0,3
PAT4	Avg	15,2	109,2	28,3	86,1	12,1	61,4	19,4	5,2	27,7	4	21,6	4,2	10,9	1,5	8,5	1,3
	Min	7,9	52,1	13,7	41,1	5,9	29,4	9,2	2,5	13,4	1,9	10,3	2	5,2	<DL	4,1	<DL
	Max	22,6	150	40	117,8	16,8	84,3	26,8	7,3	38,2	5,5	29,9	5,8	15,1	2	11,7	1,8
	SD	4,8	36,6	9,9	28,2	4	20,5	6,5	1,8	9,1	1,3	7,2	1,4	3,7	0,4	2,8	0,4
PAT5	Avg	28,6	82,8	34,1	88,9	11,5	51	14,1	3,5	20,8	2,9	16	3,2	8,4	1,3	6,8	1,2
	Min	13,6	40,2	15	39,5	5	22,8	6,2	1,6	9,4	1,4	8	1,6	4,5	<DL	3,7	<DL
	Max	69,1	203	91	240,5	32,3	138	38,9	9,4	55,9	7,6	40,6	7,9	20,6	2,8	16,3	2,4
	SD	20,3	60,6	28,6	76	10,4	43,7	12,5	3	17,6	2,4	12,4	2,4	6,1	0,7	4,8	0,6
PAT6	Avg	13,2	27,9	9,7	24,9	3,5	14,8	4,3	1,4	6,3	1,3	5,4	1,4	3,2	<DL	2,7	<DL
	Min	<DL	1,1	<DL	<DL	<DL	<DL	<DL	<DL	<DL	<DL	<DL	<DL	<DL	<DL	<DL	<DL
	Max	45,7	87,7	19,2	54,3	7,4	34	9,8	2,8	15,9	2,5	15,1	3,2	8,9	1,2	7,4	1,1
	SD	16,6	32,1	7,2	20,5	2,5	12,6	3,4	0,7	5,7	0,6	5,3	0,9	3	0,1	2,5	-
	(µg/L)	Sc	Y	La	Ce	Pr	Nd	Sm	Eu	Gd	Tb	Dy	Ho	Er	Tm	Yb	Lu
PAT7	Avg	164,5	88	44,5	111,7	14,2	53	18,1	10,1	26,1	10	19,8	10	12	10	11,7	10
	Min	69,6	44,7	24,9	62,7	10	<DL	10,9	10	14,9	10	10,4	10	10	10	10	10
	Max	270,4	175,2	86,5	228,6	26,7	110,3	34,5	10,4	50,7	10	40,1	10	21,9	10	19,9	10
	SD	64,4	44,9	21,4	59,2	6,2	35,5	8,3	0,2	12,5	0	10,4	0	4,8	0	4	0
PAT8	Avg	14,5	31,6	20,4	51	6,7	29,6	8,1	2,2	11,1	1,6	7,4	1,6	3,7	<DL	2,9	<DL
	Min	<DL	<DL	<DL	<DL	<DL	<DL	<DL	<DL	<DL	<DL	<DL	<DL	<DL	<DL	<DL	<DL
	Max	37,1	75,7	52,4	133,3	17,6	79,4	22,3	5,8	29,5	3,8	18,8	3,5	8,9	1,2	6,9	1,1
	SD	12,4	25,4	17,8	45,9	5,9	27,4	7,6	1,9	10	1,1	6,3	1	2,9	0,1	2,2	-
PAT9	Avg	7,5	18,4	12,9	31,9	4,1	17,9	4,6	1,4	6,5	1,1	4,3	1,1	2,2	<DL	1,8	<DL
	Min	1,5	3,4	2,6	5,6	<DL	3,2	<DL	<DL	1,1	<DL	<DL	<DL	<DL	<DL	<DL	<DL
	Max	11,3	28,1	20,3	51,1	6,5	29,1	7,5	1,9	10,4	1,4	6,9	1,3	3,4	<DL	2,6	<DL
	SD	4,1	10,6	7,5	19	2,4	10,8	2,7	0,4	3,9	0,2	2,5	0,1	1	-0	0,7	-
PAT10	Avg	7,1	33,6	36,3	116,2	10,5	43,3	9,3	2,6	14,4	2	7,2	1,8	3,4	1,1	2,6	1,1
	Min	<DL	6,1	4,3	10	1,2	5,4	1,3	<DL	1,9	<DL	1,2	<DL	<DL	<DL	<DL	<DL
	Max	23	149,9	177,4	604,3	51,3	208,6	43,3	10,6	68,2	7,1	32,1	5,8	14	1,8	9,8	1,5
	SD	8	57,1	69,2	239,2	20	81,1	16,7	3,9	26,4	2,5	12,2	1,9	5,2	0,3	3,6	0,2
PAT11	Avg	4,6	20	15,8	33,2	4	16,1	3,9	1,3	5,8	1,2	3,7	1,1	2	<DL	1,6	<DL
	Min	1,6	3,8	<DL	<DL	<DL	<DL	<DL	<DL	<DL	<DL	<DL	<DL	<DL	<DL	<DL	<DL
	Max	12,4	38,5	55,8	102,9	11,6	45,9	9,2	2,4	15,1	1,7	8,1	1,5	3,6	<DL	2,7	<DL
	SD	4,1	15,4	20,6	37,9	4,1	16,9	3,3	0,5	5,6	0,3	3,1	0,2	1,2	-	0,8	-
PAT12	Avg	1,1	<DL	<DL	<DL	<DL	<DL	<DL	<DL	<DL	<DL	<DL	<DL	<DL	<DL	<DL	<DL
	Min	<DL	<DL	<DL	<DL	<DL	<DL	<DL	<DL	<DL	<DL	<DL	<DL	<DL	<DL	<DL	<DL
	Max	1,4	<DL	<DL	<DL	<DL	<DL	<DL	<DL	<DL	<DL	<DL	<DL	<DL	<DL	<DL	<DL
	SD	0,2	-	-	-	-	-	-	-	-	-	-	-	-	-	-	-

**Table 2**

Spearman correlation matrix using some typical variables of AMD and host rocks.

	REE	pH	SO <sub>4</sub>	Fe	Al	Mn	Acidez
REE	1	-0,909	0,923	0,909	0,888	0,986	0,907
pH	-0,909	1	-0,902	-0,944	-0,951	-0,916	-0,942
SO <sub>4</sub>	0,923	-0,902	1	0,958	0,965	0,951	0,97
Fe	0,909	-0,944	0,958	1	0,979	0,93	0,984
Al	0,888	-0,951	0,965	0,979	1	0,909	0,991
Mn	0,986	-0,916	0,951	0,93	0,909	1	0,921
Acidez	0,907	-0,942	0,97	0,984	0,991	0,921	1

(e.g., Verplanck et al., 2004; Sun et al., 2012; Stewart et al., 2017). However, this is not always the case. For example, PAT7 has the lowest pH, but the highest concentrations of Σ(REE) occurs in PAT2, with 888.2 µg/L. These results can be related to the possible sources of these elements. Firstly, the REE can be originated from inherited materials, that is, be part of the host rocks; and secondly, they can be linked to the mineral-water interaction processes associated with AMD. Thus, it is

possible that in PAT2 (the pit lake) these two origins can be found, while in PAT7 (acidic pond) REE are more dependent on the high amounts of reactive materials in the surroundings. According to several authors (e.g., Migaszewski et al., 2014; Cánovas et al., 2019), bedrock mineralogy and lithology are strongly linked to REE concentrations, in AMD contexts.

The abundance of REE in sites within the mining complex (especially

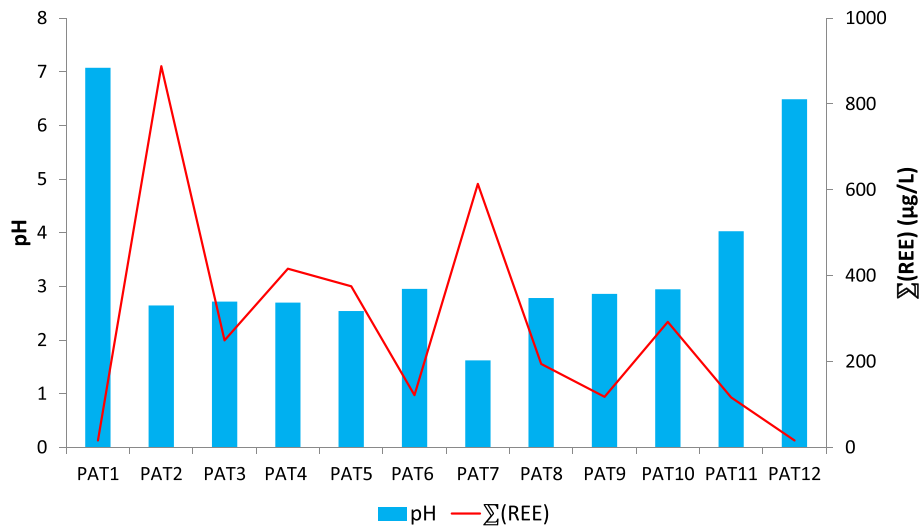


Fig. 5. Variation of the average pH values and average sum of REE in water samples along São Domingos River system, observed for the six campaigns.

in acidic lagoons) exceeded, by 2–3 times the order of magnitude, the ones in neutral freshwaters (PAT1 and PAT12). The same has been noticed by Da Silva et al. (2009), when they analyzed a mining system, also located in the IPB. However, and according to Migaszewski and Galuszka (2015), this range of values is commonly observed in AMD environments, where they are expressed in tens to hundreds of µg/L.

#### 4.2. Source of REE

To better understand the origin of REEs, multivariate statistical analysis was applied to explore their interrelationships with the factors that may affect their behavior in AMD (Table 2). For statistical analysis, the average concentration of all elements (ΣREEs) was used.

The REE have high correlations (>0.90) with the typical elements of AMD and the host rocks of the region. Therefore, as observed by Saeedi et al. (2012), the results indicate that these elements may have a common origin, mutual dependence, and similar behavior during transport. Thus, the REE have the same provenance as the enclosing rock elements and were mobilized by processes leading to AMD. This is suggested by the relationship of REE with sulfate and acidity (typical indicators of AMD). According to Nesbitt (1979), REE can be released from primary minerals (e.g., feldspars) and then adsorbed by secondary phases. Furthermore, AMD involves a wide variety of inorganic compounds with high capacity to participate in complexation reactions that can play an

important role in the fractionation of REE, such as sulfate (Zhao et al., 2007). In addition, the acidic conditions promoted by pyrite oxidation favored the dissolution of minerals in waste-dumps. Consequently, this contributes to high soluble concentrations of REEs, sulfates, Mg, Fe, Mn, and Al.

The results of the factor analysis (Fig. 6) reveal a similar behavior demonstrated by the correlation analysis. Therefore, as in Xu et al. (2018), there is high affinity between REEs, SO<sub>4</sub><sup>2-</sup>, Fe, Mn, Al, and acidity, corresponding to the positive part of factor 1. It is known that SO<sub>4</sub>, Al, Fe, and acidity are strongly linked to AMD processes. The pH, on the other hand, is at the negative side of the axis corresponding to factor 2, being at the opposite extreme to REE. These results agree with those obtained in Fig. 5, which demonstrated the inverse relationship between these two components. These variables are directly related to the dissolution of enclosing rocks and the weathering processes resulting from contact with water and oxygen, to which the materials in waste-dumps are subject. Cánovas et al. (2019), that studied the Spanish sector of the IPB, with a similar geological context, described that the main factor that control the REE concentrations, is the intensity of AMD in the weathering of host rocks.

#### 4.3. Normalized REE standards

The analysis of the REE was performed only with samples collected

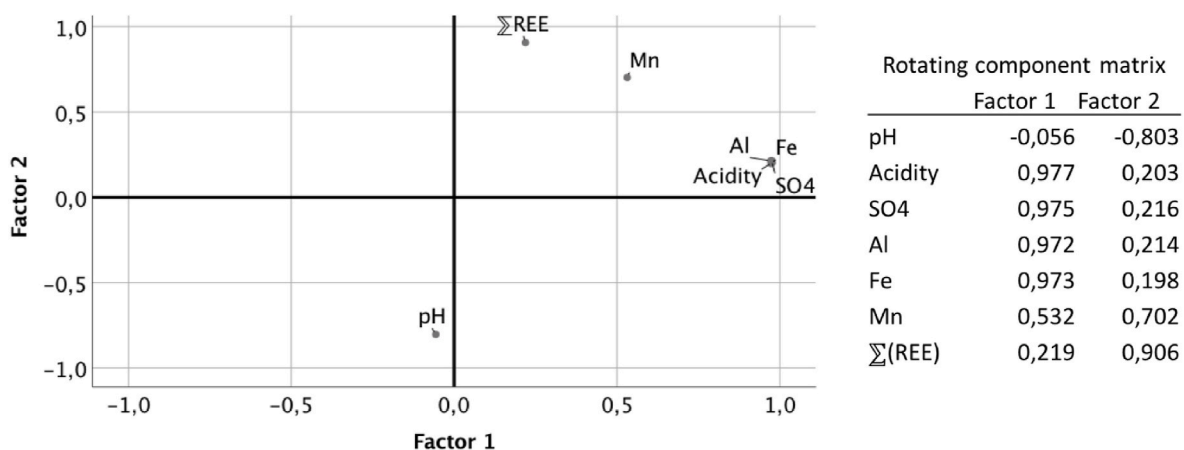


Fig. 6. Results of factor analysis. Extraction Method: Principal Component Analysis; Rotation Method: Varimax with Kaiser Normalization; Rotation converged in three iterations.

in sites with obvious manifestations of mining contamination (from PAT2 to PAT11), thus excluding points PAT1 and PAT12, characterized above as clean water.

The graph in Fig. 7 shows the concentration of these elements throughout the mining system.

Normalization expresses a clear convex curvature in the MREE when compared to the LREE and HREE. In general, it is possible to observe that most samples show enrichment in MREE ( $Gd_n/Lu_n$ ), like the signature observed by Soyol-Erdene et al. (2018). This fact had also already been reported by Pérez-López et al. (2010), when studying various materials in this mining area. The sites PAT9, PAT2, PAT8, and PAT11 deserve special mention. It should be noted that PAT9 and PAT11 present signs of lower contamination (by metals, sulfate, acidity) when compared to other sampling sites. Also, these are characterized as being the sites with the lowest sum of REE (117.4 and 116.4  $\mu\text{g/L}$ , respectively). However, and according to Leybourne and Johannesson (2008), an enrichment of MREE is likely to be observed also in non-acidic waters that contain high concentrations of organic matter and colloids. Indeed, colloidal material was observed along the two streams that run through the mining complex, being marked in PAT8 and PAT11 (Fig. 2). Also, the occurrence of acidophilic algae blooms (Gomes et al., 2021) should contribute to the presence of organic matter at these sites. Therefore, this enrichment could occur under diverse conditions (e.g., Welch et al., 2009; Prudêncio et al., 2015).

In the PAAS-normalized pattern, PAT2 presents a positive anomaly for Ce and PAT3 a negative anomaly for Yb. In the latter case, and according to Soyol-Erdene et al. (2018), Yb is likely retained by AMD-precipitates. Gomes et al. (2017a, b) had already reported the presence of numerous saline efflorescences in this location, mainly Fe, Mg and Al-sulfates, able to retain this element, as demonstrated by Soyol-Erdene et al. (2018).

On the other hand, the sampling sites with the lowest normalized concentration (Fig. 7) are, in general, PAT4, PAT7 and PAT5, characterized, the latter two, by extreme hydrochemical conditions. The fact that AMD-precipitates are very abundant in PAT7, may be an explanation for this behavior. According to Merten et al. (2005), mineral precipitation and the presence of pyrite ash (observed and identified in the work by Gomes et al., 2017a), may favor the incorporation of REE elements, namely LREE in saline neoformations.

High concentrations of REE can lead to ecotoxicity problems, such as disruption of bone integrity, competition between La and Ca or Mg, substitution of Fe by Sc, and phosphate deficiency (Gonzalez et al.,

2014). Thus, evaluating the distributions, concentrations and possible environmental impacts of REEs in mining regions influenced by AMD catalytic processes can play a preponderant role in ecotoxicology. Therefore, it helps to support future decisions regarding water quality management. Furthermore, weathering, mineral dissolution, secondary dispersion, precipitation of Fe oxyhydroxides, sulfate efflorescences and metal adsorption on neoformed minerals can contribute to the geochemical recycling of REE and other PTE (Nordstrom, 1982).

## 5. Conclusion

The reservoir upstream of the mining area (PAT1) represents clean water, without evidence of contamination, namely regarding the typical AMD indicators (pH, EC, sulfate, and acidity), and concentration of REE. The samples corresponding to the pit lake (PAT2) and acidic lagoons (PAT 3 to PAT 10) had mean pH values below 3, which confirms the influence of leachates from sulfide-rich wastes on the water quality. From the point of dispersion of the AMD plume in the river (PAT 11) and subsequent PAT 12, there is a tendency for an increase in pH and a decrease in EC. This trend is provided by the higher distance from the waste accumulations, and consequent natural attenuation, for example, by dilution and retention of pollutants on AMD-precipitates.

The abundance of REE in mine waters exceeds that of normal freshwaters by 2–3 times the order of magnitude. In addition to the above, within the mining complex, there are locations with very high concentration of REE, specifically represented by the points PAT2 and PAT7. The concentrations of the REE increase as the pH of the water decreases. Thus, these elements may originate in the host rocks, being also linked to the weathering processes associated with AMD.

Most samples show enrichment in MREE ( $Gd_n/Lu_n$ ), similarly to the classic signature of AMD. In turn, colloids and AMD-precipitates may also be retaining these elements.

Future direction of research should consider two topics related with mine waters and REE: (i) critical nature of REE as strategic raw materials and its potential recovery from the most contaminated waters and wastes; (ii) Climate disruptions with increasingly frequent and persistent droughts. Climate change may be influencing biogeochemical processes and hydrological cycles. In this sense, the impact of REE is a matter of relevant interest in upcoming studies, especially in water scarcity situations, that may help to support decisions related to water quality management.

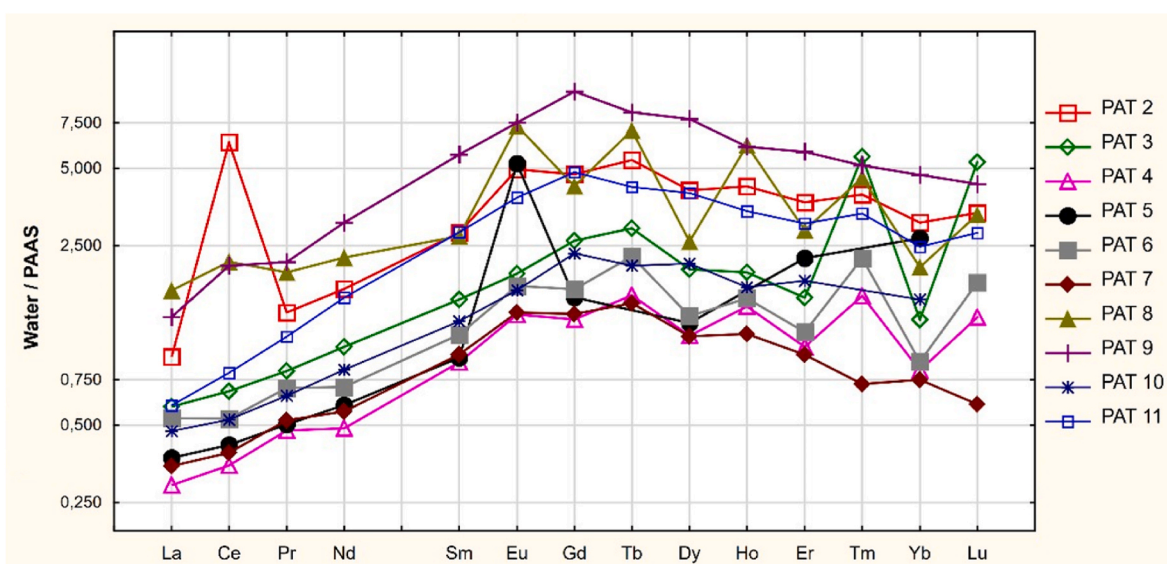


Fig. 7. PAAS-normalized REE patterns for water samples during the rainy season.



## Credit author statement

Patrícia Gomes – Conceptualization, formal analysis, writing—original draft, investigation. Teresa Valente – Supervision, Conceptualization, methodology, formal analysis, Writing - Review & Editing, investigation. Rosa Marques - writing—original draft, investigation. Maria Isabel Prudêncio - Supervision, writing—original draft, investigation, Writing - Review & Editing. Jorge Pamplona – writing—original draft, investigation, Visualization, Writing - Review & Editing. All authors have read and agreed to the published version of the manuscript.

## Declaration of competing interest

The authors declare that they have no known competing financial interests or personal relationships that could have appeared to influence the work reported in this paper.

## Data availability

The data that has been used is confidential.

## Acknowledgments

Patrícia Gomes acknowledges FCT (Science and Technology Foundation, Portugal) by the research fellowship under the POCH (Programa Operacional Capital Humano) supported by the European Social Fund and National Funds of MCTES (Ministério da Ciência, Tecnologia e Ensino Superior) with reference SFRH/BD/108887/2015. This work was co-funded by FCT through projects UIDB/04683/2020, UIDP/04683/2020 and Nano-MINENV 029259 (PTDC/CTAAMB/29259/2017). The authors are grateful to the anonymous reviewers for their valuable contributions to improving the manuscript.

## References

- Anawar, H., 2015. Sustainable rehabilitation of mining waste and acid mine drainage using geochemistry, mine type, mineralogy, texture, ore extraction and climate knowledge. *J. Environ. Manag.* 158, 111–121. <https://doi.org/10.1016/j.jenvman.2015.04.045>.
- ASTM, 1992. D 5425-92 - Standard Practice for Cleaning Laboratory Glassware, Plasticware and Equipment Used in Microbiological Analysis. ASTM Committee on Standards, American Society for Testing and Materials, p. 5.
- Åström, M., Corin, N., 2003. Distribution of rare earth elements in anionic, cationic and particulate fractions in boreal humus-rich streams affected by acid sulphate soils. *Water Res.* 37, 273–280.
- Balaram, V., 2019. Rare earth elements: a review of applications, occurrence, exploration, analysis, recycling, and environmental impact. *Geosci. Front.* 10, 1285–1303. <https://doi.org/10.1016/j.gsf.2018.12.005>.
- Batista, M.J., 2000. Environmental State in the Portuguese Test Site S. Domingos Mine: Past and Present Report European Commission. Available in: [http://www.brgm.fr/mineo/IGM\\_test\\_site.pdf](http://www.brgm.fr/mineo/IGM_test_site.pdf).
- Cánovas, C.R., Chapron, S., Arrachart, G., Pellet-Rostaing, S., 2019. Leaching of rare earth elements (RREs) and impurities from phosphogypsum: a preliminary insight for further recovery of critical raw materials. *J. Clean. Prod.* 219, 225–235. <https://doi.org/10.1016/j.jclepro.2019.02.104>.
- Cordeiro, M., 2017. MSc thesis. In: *Caracterização ambiental do complexo mineiro de São Domingos – cartografia de infra-estruturas e impacto sobre o meio hídrico*. University of Minho, Braga, p. 84p [abstract in English].
- Costis, S., Mueller, K., Coudert, L., Neculita, C., Reynier, N., Blais, J., 2021. Recovery potential of rare earth elements from mining and industrial residues: a review and cases studies. *J. Geochem. Explor.* 221, 106699 <https://doi.org/10.1016/j.gexplo.2020.106699>.
- Da Silva, Bobos, I., Matos, J.X., Patinha, C., Reis, A.P., Fonseca, E.C., 2009. Mineralogy and geochemistry of trace metals and REE in volcanic massive sulfide host rocks, stream sediments, stream waters and acid mine drainage from the Lousal mine area (Iberian Pyrite Belt, Portugal). *Appl. Geochem.* 24 (3), 383–401. <https://doi.org/10.1016/j.apgeochem.2008.12.001>.
- Delgado, J., Pérez-López, R., Galván, L., Nieto, J.M., Boski, T., 2012. Enrichment of rare earth elements as environmental tracers of contamination by acid mine drainage in salt marshes: a new perspective. *Mar. Pollut. Bull.* 64, 1799–1808.
- Dold, B., 2014. Evolution of acid mine drainage formation in sulphidic mine tailings. *Minerals* 4, 621–641. <https://doi.org/10.3390/min4030621>.
- Du, X., Graedel, T.E., 2011. Uncovering the global life cycles of the rare earth elements. *Sci. Rep.* 1, 145. <https://doi.org/10.1038/srep00145>.
- Dukov, I., 2007. Nomenclature of Inorganic Chemistry – IUPAC Recommendations 2005, vol. 16, pp. 561–568.
- El Rasafi, T., Nouri, M., Haddioui, A., 2021. Metals in mine wastes: environmental pollution and soil remediation approaches – a review. *Geosyst. Eng.* 24, 157–172. <https://doi.org/10.1080/12269328.2017.1400474>.
- EPA, 2012. Guidelines for Water Reuse. EPA/600/R-12/618, September.
- Fernández-Caliani, J.C., Barba, C., González, I., Galán, E., 2009. Heavy metal pollution in soils around the abandoned mine sites of the Iberian Pyrite Belt (Southwest Spain). *Water Air Soil Pollut.* 200, 211–226. <https://doi.org/10.1007/s11270-008-9905-7>.
- Galhardi, J., Luko-Sulato, K., Yabuki, L., Santos, L., da Silva, Y., da Silva, Y.J.B., 2022. In: Dalu, T., Tavengwa, N.T. (Eds.), Chapter 17 - Rare Earth Elements and Radionuclides. Elsevier, pp. 309–329. <https://doi.org/10.1016/B978-0-12-822850-0.00011-9>.
- García-Lorenzo, M.L., Marimo, J., Navarro-Hervas, M.C., Perez-Sirvent, C., Martínez-Sánchez, M.J., Molina-Ruiz, J., 2016. Impact of acid mine drainages on surficial waters of an abandoned mining site. *Environ. Sci. Pollut. Res. Int.* 23, 6014–6023. <https://doi.org/10.1007/s11356-015-5337-2>.
- Gomes, P., 2011. *Processos de Reabilitação Natural em Escombreiras de Minas Abandonadas - Estudo de Casos*. Master's Thesis. University of Porto, Porto, p. 121p [abstract in English].
- Gomes, P., 2021. *Impact of Acid Mine Drainage on the Environmental Quality and Potential Accumulation of Strategic Metals in Water Dams Located in the Iberian Pyrite Belt*. PhD thesis. Univ. Minho, Braga, p. 319p.
- Gomes, P., Valente, T., Grande, J.A., Cordeiro, M., 2017a. Occurrence of sulphate efflorescences in São Domingos mine. *Comunicações Geológicas* 104 (1), 0873-948X; e-ISSN: 1647- 581X.
- Gomes, P., Valente, T., Grande, J.A., Cordeiro, M., 2017b. Relationships between Physico-Chemical Indicator of Acid Mine Drainage. XII Congresso Nacional de Geoquímica/XI Congresso Ibérico de Geoquímica, Linares, pp. 114–118, 26 - 28 september.
- Gomes, P., Valente, T., Pereira, P., 2018. Addressing quality and usability of surface water bodies in semi-arid regions with mining influences. *Environ. Process.* 5, 707. <http://doi:10.1007/s40710-018-0329-0>.
- Gomes, P., Valente, T., Geraldo, D., Ribeiro, C., 2020. Photosynthetic pigments in acid mine drainage: seasonal patterns and associations with stressful abiotic characteristics. *Chemosphere* 239, 124774. <https://doi.org/10.1016/j.chemosphere.2019.124774>.
- Gomes, P., Valente, T., Albuquerque, T., Henriques, R., Flor-Arnau, N., Pamplona, J., Macías, F., 2021. Algae in acid mine drainage and relationships with pollutants in a degraded mining ecosystem. *Minerals* 11, 110. <https://doi.org/10.3390/min11020110>.
- Gonzalez, V., Vignati, D.A.L., Leyval, C., Giamberini, L., 2014. Environmental fate and ecotoxicity of lanthanides: are they a uniform group beyond chemistry? *Environ. Int.* 71, 148–157.
- González, R., Cánovas, C., Olías, M., Macías, F., 2020. Rare earth elements in a historical mining district (south-west Spain): hydrogeochemical behaviour and seasonal variability. *Chemosphere* 253, 126742. <https://doi.org/10.1016/j.chemosphere.2020.126742>.
- Grawunder, A., Merten, D., Büchel, G., 2014. Origin of middle rare earth element enrichment in acid mine drainage-impacted areas. *Environ. Sci. Pollut. Res. Int.* 21, 6812–6823.
- Gwenzi, W., Mangori, L., Danha, C., Chaukura, N., Dunjana, N., Sanganyado, E., 2018. Sources, behaviour, and environmental and human health risks of high-technology rare earth elements as emerging contaminants. *Sci. Total Environ.* 636, 299–313.
- He, Z.L., Shentu, J., Yang, X.E., 2010. Manganese and selenium. In: Hooda, P.S. (Ed.), *Trace Elements in Soils*. John Wiley & Sons Ltd, United Kingdom, pp. 481–497.
- Hermassi, M., Granados, M., Valderrama, C., Ayora, C., Cortina, J.L., 2022. Recovery of rare earth elements from acidic mine waters: an unknown secondary resource. *Sci. Total Environ.* 810, 152258 <https://doi.org/10.1016/j.scitotenv.2021.152258>.
- Huang, X.C., Zhang, G., Pan, A.F., Chen, F., Zheng, C., 2016. Protecting the environment and public health from rare earth mining. *Earth Future* 4, 532–535.
- Kulaksiz, S., Bau, M., 2007. Contrasting behaviour of anthropogenic gadolinium natural rare earth elements in estuaries and the gadolinium input into the North Sea. *Earth Planet Sci. Lett.* 260, 361–371.
- Kurvet, I., Juganson, K., Vija, H., Sihtmäe, M., Blinova, I., Svyrtens-Wiig, J., Kahru, A., 2017. Toxicity of nine (doped) rare earth metal oxides and respective individual metals to aquatic microorganisms *Vibrio fischeri* and *Tetrahymena thermophila*. *Materials* 10, 754. <https://doi.org/10.3390/ma10070754>.
- Leybourne, M.L., Johannesson, K.H., 2008. Rare earth elements (REE) and yttrium in stream waters, stream sediments and Fe-Mn oxyhydroxides: fractionation, speciation and controls over REE+Y patterns in the surface environments. *Geochem. Cosmochim. Acta* 72, 5962–5983.
- Li, X., Wu, P., 2017. Geochemical characteristics of dissolved rare earth elements in acid mine drainage from abandoned high-As coal mining area, southwestern China. *Environ. Sci. Pollut. Res.* 24, 20540–20555. <https://doi.org/10.1007/s11356-017-9670-5>.
- Massari, S., Ruberti, M., 2013. Rare earth elements as critical raw materials: focus on international markets and future strategies. *Resour. Pol.* 38, 36–43.
- Matos, J.X., 2004. *Carta geológico-mineira de São Domingos*. Instituto Geológico e Mineiro, Lisboa.
- Matos, J.X., Martins, L.P., 2006. Reabilitação ambiental de áreas mineiras do sector português da Faixa Piritosa Ibérica: estado da arte e perspectivas futuras. *Bol. Geol. Min.* 11, 289–304.
- Matos, J.X., Soares, S., Claudino, C., 2006a. *Caracterização Geológica-Geotécnica da corta da mina de São Domingos*. FPI. X Congresso Nacional de Geotecnia. SPG/UNL 3, 741–752.

- Matos, J.X., Pereira, Z., Oliveira, V., Oliveira, J.T., 2006b. The Geological Setting of the São Domingos Pyrite Orebody, Iberian Pyrite Belt. VII Congresso Nacional de Geologia, Universidade de Évora, Évora.
- Matos, J.X., Pereira, Z., Batista, M.J., Oliveira, D.D., 2012. São Domingos mining site - Iberian pyrite Belt. In: 9th International Symposium on Environmental Geochemistry, pp. 7–12.
- Merten, D., Geletneky, J., Bergmann, H., Haferburg, G., Kothe, E., Buchel, G., 2005. Rare earth element patterns: a tool for understanding processes in remediation of acid mine drainage. *Chemie der Erde – Geochem.* 5, 97–114.
- Migaszewski, Z.M., Galuszka, A., 2015. The characteristics, occurrence, and geochemical behavior of rare earth elements in the environment: a review. *Crit. Rev. Environ. Sci.* 45, 429–471.
- Migaszewski, Z., Galuszka, A., Migaszewski, A., 2014. The study of rare earth elements in farmer's well waters of the Podwisniówka acid mine drainage area (south-central Poland). *Environ. Monit. Assess.* 186, 1609–1622. <https://doi.org/10.1007/s10661-013-3478-7>.
- Moreno-González, R.M., Macías, F., Olías, M., Canovas, C.R., 2022. Temporal evolution of acid mine drainage (AMD) leachates from the abandoned Tharsis mine (Iberian Pyrite Belt, Spain). *Environ. Pollut.* 295, 118697 <https://doi.org/10.1016/j.envpol.2021.118697>.
- Nesbitt, H.W., 1979. Mobility and fractionation of rare elements during weathering of a granodiorite. *Nature* 279, 206–210.
- Noack, C.W., Dzombak, D.A., Karamalidis, A.K., 2014. Rare earth element distributions and trends in natural waters with a focus on groundwater. *Environ. Sci. Technol.* 48, 4317–4326.
- Nordstrom, D.K., 1982. Aqueous pyrite oxidation and the consequent formation of secondary iron minerals. In: Fanning, D.S., Hossner, L.R., Kittrick, J.A. (Eds.), *Acid Sulfate Weathering*. Soil Science Society of America, Madison, WI, pp. 37–56.
- Olías, M., Cerón, J., Fernández, I., De la Rosa, J., 2005. Distribution of rare earth elements in an alluvial aquifer affected by acid mine drainage: the Guadiamar aquifer (SW Spain). *Environ. Pollut.* 135, 53–64.
- Oliveira, J.T., Matos, J.X., 2004. O caminho de ferro da Mina de S. Domingos ao Pomarão: um percurso geoducacional na Faixa Piritosa Ibérica. XXIV Encontro Prof. Geociências, APG, p. 19.
- Pérez-López, R., Deado, J., Nieto, J.M., Márquez-García, B., 2010. Rare earth element geochemistry of sulphide weathering in the Sao Domingos mine area (Iberian Pyrite Belt): a proxy for fluid-rock interaction and ancient mining pollution. *Chem. Geol.* 276, 29–40.
- Protano, G., Riccobono, F., 2002. High contents of rare earth elements (REEs) in stream waters of a Cu–Pb–Zn mining area. *Environ. Pollut.* 117, 499–514.
- Prudêncio, M.I., Valente, T., Marques, R., Sequeira Braga, M.A., Pamplona, J., 2015. Geochemistry of rare earth elements in a passive treatment system built for acid mine drainage remediation. *Chemosphere* 138, 691–700.
- Rim, K., 2016. Effects of rare earth elements on the environment and human health: a literature review. *Toxicol. Environ. Health. Sci.* 8, 189–200.
- Saeedi, M., Li, L.Y., Salmanzadeh, M., 2012. Heavy metals and polycyclic aromatic hydrocarbons: pollution and ecological risk assessment in street dust of Tehran. *J. Hazard Mater.* 227–228, 9–17.
- Sahoo, P.K., Tripathy, S., Equeenuddin, S.M., Panigrahi, M.K., 2012. Geochemical characteristics of coal mine discharge vis-a-vis behavior of rare earth elements at Jaintia Hills coalfield, northeastern India. *J. Geochem. Explor.* 112, 235–243.
- Sharifi, R., Moore, F., Keshavarzi, B., 2013. Geochemical behavior and speciation modeling of rare earth elements in acid drainages at Sarcheshmeh porphyry copper deposit, Kerman Province, Iran. *Chemie der Erde – Geochem.* 73, 509–517.
- Soyol-Erdene, T.O., Valente, T., Grande, J.A., de la Torre, M.L., 2018. Mineralogical controls on mobility of rare earth elements in acid mine drainage environments. *Chemosphere* 205, 317–327. <https://doi.org/10.1016/j.chemosphere.2018.04.095>.
- Stewart, B.W., Capo, R.C., Hedin, B.C., Hedin, R.S., 2017. Rare earth element resources in coal mine drainage and treatment precipitates in the Appalachian Basin, USA. *Int. J. Coal Geol.* 169, 28–39.
- Sun, H., Zhao, F., Zhang, M., Li, J., 2012. Behavior of rare earth elements in acid coal mine drainage in Shanxi Province, China. *Environ. Earth Sci.* 67, 205–213.
- Tao, Y., Shen, L., Feng, C., Yang, R., Qu, J., Ju, H., Zhang, Y., 2022. Distribution of rare earth elements (REEs) and their roles in plant growth: a review. *Environ. Pollut.* 298, 118540 <https://doi.org/10.1016/j.envpol.2021.118540>.
- Taylor, S.R., McLennan Blackwell, S.M., 1985. *The Continental Crust: its Composition and Evolution*. Taylor and McLennan, Oxford.
- Thornton, I., 1996. Impacts of mining on the environment: some local, regional and global issues. *Appl. Geochem.* 11, 355–661.
- Valente, T., Gomes, P., Pamplona, J., de la Torre, M.L., 2012. Natural stabilization of mine waste-dumps - evolution of the vegetation cover in distinctive geochemical and mineralogical environments. *J. Geochem. Explor.* 123, 152–161. <https://doi.org/10.1016/j.gexplo.2012.05.005>.
- Valente, T., Grande, J.A., de la Torre, M.L., Gomes, P., Santisteban, M., Borrego, J., Sequeira Braga, M.A., 2015. Mineralogy and geochemistry of a clogged mining reservoir affected by historical acid mine drainage. *Geochem. Explor.* 157, 66–76.
- Verplanck, P.L., Nordstrom, D.K., Taylor, H.E., Kimball, B.A., 2004. Rare earth element partitioning between hydrous ferric oxides and acid mine water during iron oxidation. *Appl. Geochem.* 19, 1339–1354. <https://doi.org/10.1016/j.apgeochem.2004.01.016>.
- Welch, S.A., Christy, A.G., Isaacson, L., Kirste, D., 2009. Mineralogical control of rare earth elements in acid sulfate soils. *Geochem. Cosmochim. Acta* 73, 44–64.
- Xu, N., Morgan, B., Rate, A.W., 2018. From source to sink: rare-earth elements trace the legacy of sulfuric dredge spoils on estuarine sediments. *Sci. Total Environ.* 637–638, 1537–1549.
- Zhang, W., Honaker, R., 2020. Process development for the recovery of rare earth elements and critical metals from an acid mine leachate. *Miner. Eng.* 153, 106382 <https://doi.org/10.1016/j.mineng.2020.106382>.
- Zhao, F., Cong, Z., Sun, H., Ren, D., 2007. The geochemistry of rare earth elements (REE) in acid mine drainage from the Sitai coal mine, Shanxi Province, North China. *Int. J. Coal Geol.* 70, 184–192.